Sufficient Node Density Conditions on Delay-Tolerant Sensor Networks for Wildlife Tracking and Monitoring

Samina Ehsan, Max Brugger, Kyle Bradford, Bechir Hamdaoui, Yevgeniy Kovchegov
Oregon State University, Corvallis, Oregon, USA
ehsans, bruggerm, bradfork, hamdaoub, kovchegy@onid.orst.edu

***Abstract*— This paper investigates the performance limits of delay tolerant networks (DTNs) with intermittently connected nodes deployed for wildlife monitoring, wherein information is either transmitted or carried to static access-points by free-ranging animals whose movement is assumed to be random. Specifically, in such mobility-aided applications where routing is performed in a store-carry-and-drop manner, limited buffer capacity of a carrier node plays a critical role, and data loss due to buffer overflow heavily depends on access-point density. Driven by this fact, our focus in this paper is on providing sufficient conditions on access-point density that limit the likelihood of buffer overflow. Specifically, we first derive and prove sufficient access-point density conditions that ensure that the data loss rates are statistically guaranteed to be below a given threshold. We consider studying both the square and hexagonal access-point deployment structures. Then, we validate the derived theoretical results for each of the two studied structures through simulations.**

I. Introduction

The deployment of extremely versatile sensor networks in a variety of real world applications is progressing from concept to reality. Wildlife monitoring is an important example that has received considerable attention during the last decade. Biologists have long recognized the need for insight into animal habitat, the monitoring of endangered species, and the study of socialization behavior in animals, as these are all necessary to understand their physiology, behavior, and ecology. However, many species are rare and wide-ranging, and thus difficult to monitor directly or capture for repetitive physiological measures [1]. During the last decade, researchers have been designing automated monitoring systems which demand less human presence in the field. After initial attempts which, at times, provided inconsistent and invalid outcomes, efforts have been made on the deployment of enormously potent sensor networks for this kind of application [2, 3].

In sensor networks, free-ranging animals are equipped with light-weight battery-powered collars, attached at the neck. The collars are designed to operate inconspicuously, collecting and saving spatio-temporal data (for example, location information, biometric, and activity information, etc.) continuously, without disrupting the animal's normal activities. At regular intervals, the collar (having a relatively limited memory space) transmits its data to a device where data storage is not an issue. However, due to the continuous and random movement of the animals, fixed network infrastructure cannot be used for data transmission. And, due to the lack of continuous connectivity, traditional MANET techniques cannot be applied either. Attempts have been focused instead on store-carry-and-drop routing to static access points [4], where transmission occurs when the animal is in close proximity to the fixed node. A special class of sensor networks, known as delay tolerant networks (DTNs), is considered to be well suited for these wildlife monitoring applications that are typically underserved by traditional networks [5–10].

Such DTNs are sparse networks of mobile nodes, equipped with buffers of limited capacity, and static access-points with virtually unlimited buffer capacity. Since every mobile node in the network stores an amount of data that increases with time, and there is no guarantee of when mobile nodes will reach the coverage area (the area surrounding the access-point where data transfer can be performed), the buffer may overflow frequently, leading to data loss which severely hampers the reliability of the system. It is important to understand how the reliability of such networks depends on the density of the static nodes, as this density relates to both the frequency with which a mobile node visits coverage areas and the probability of buffer overflow. Although considerable research efforts have focused on protocol design [11–14], connectivity analysis [15, 16], delay modeling and characterization [17, 18], and mobility analysis [19, 20], the effect of access-point density on data loss is still not well-understood.

In this paper, we propose sufficient conditions on access-point density of partially covered, intermittently connected DTNs deployed for wildlife monitoring/tracking so that the data loss rate does not exceed a given threshold. To the best of our knowledge, there is no previous work addressing the issue of critical density from this perspective. Due to the limited coverage (the network is disconnected in the traditional sense), data delivery is only possible through animals whose movement is assumed

random (henceforth referred to as mobile nodes), which store and carry data until they come close to a fixed node with no power constraints (henceforth referred to as an access-point), where data is then fully downloaded. The focus of this work is then on partially connected networks where both the node density and the coverage ratio are assumed to be low. In this work, we derive theoretic sufficient conditions on the access-point density, ensuring that data loss rates are statistically guaranteed to be below a given data loss threshold.

We explore two two-dimensional (2-D) access point deployment structures: the square grid and the hexagon grid. We use a mathematical model based on Brownian Motion to analyze the movement of mobile carrier nodes. In particular, the contribution of this paper is threefold:

- Derivation of sufficient access-point density conditions of partially covered, intermittently connected DTNs, consisting of both mobile and static nodes, deployed for wildlife monitoring, to ensure that data loss rates are bounded by a given threshold;
- Asymptotic behavioral analysis of the access-point density when varying the buffer size and/or data loss rate threshold; and
- Validation of the derived theoretical results through intensive simulations.

The rest of the paper is organized as follows. In Section II, we present our network model. We then derive in Section III sufficient bounds on access-point density. In Section IV, we validate our theoretical results via simulation. Finally, we conclude the paper in Section V.

II. Network Model

We consider a delay-tolerant sensor network used for tracking and monitoring free-ranging animals in their natural environment. For this, we assume and study DTNs that can experience long data transmission delays and frequent disconnection, and that consist of access-points laid out on a grid structure and a set of mobile nodes (animals). We assume that mobile nodes in these sensor networks independently and continuously generate data (for example, the animal's position and speed) at rate c. Whenever a mobile node comes within the coverage area of an access-point, it immediately and completely downloads its generated data. Each mobile node is assumed to be equipped with a memory chip that has a buffer with limited size of B bits, and when the buffer is full the newly generated data is dropped. Let $\tau = B/c$, which basically represents the minimum amount of time required to overflow the buffer of the mobile node. Also, let $\bar{\epsilon}$ denote the data loss rate threshold that mobile nodes can tolerate.

In these sensor networks, mobile nodes rely on their mobility to maintain connectivity with the access-points as the networks are only partially covered by the access-points and the coverage ratio is relatively low. Throughout this paper, we assume that the *coverage ratio*[1] is low; all the mathematical analysis and derivation provided in this paper depends on this assumption.

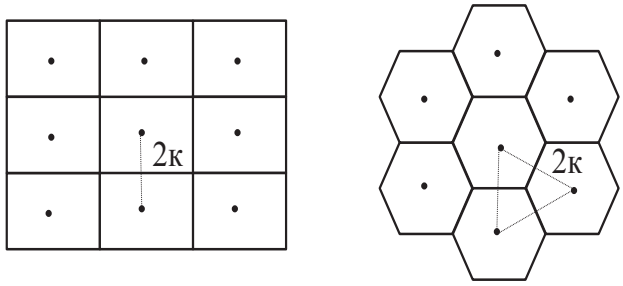

Fig. 1. Each access-point has a communication disk of radius ρ surrounding it, and is distance 2κ away from its four closest neighbors in the square grid deployment structure and its six closest neighbors in the hexagon grid deployment structure.

We consider node deployment structures where access-points are placed via a grid structure, and mobile nodes are free to move within the plane—their paths are modeled by a 2-D Brownian Motion. In this paper, we study two node deployment structures: the square grid and the hexagon grid. In the square grid structure, shown in Fig. 1 (left), each access-point is surrounded by four access-points of distance 2κ away. We assume that each access-point is surrounded by a communication disk of radius ρ. We draw a square around each access-point, of side length 2κ, and note that if an animal is anywhere in the square, the access-point at the center is its closest access-point. Thus,the node density, ν, and coverage ratio, η, can respectively be expressed as $1/(4\kappa^2)$ and $\pi\rho^2/(4\kappa^2)$.

In the hexagon grid structure, shown in Fig. 1 (right), access-points are placed in the plane to form a hexagon grid—each access point is surrounded by six access-points in each direction, each 2κ away. We identify an arbitrary point's closest access-point by drawing a hexagon around each access-point. We assume that each access-point is surrounded by a small communication disk of radius ρ, and that each hexagon has *apothem* κ, where the *apothem* is defined to be the length of the shortest line from the center to an edge (the radius is the length of the longest such line). In the hexagon grid structure, the node density ν and the coverage ratio η can be expressed as $1/(2\sqrt{3}\kappa^2)$ and $\pi\rho^2/(2\sqrt{3}\kappa^2)$, respectively.

III. Access-Point Density Analysis

It is clear that the density of access-points in a given network affects the data loss rate of a mobile node. In this work, we derive and provide sufficient conditions on the access-point density to ensure that the data loss rate does not exceed a given threshold. Before proceeding with

[1]The coverage ratio is defined as the fraction of the area covered by access-points' communication ranges relative to that of the network area.

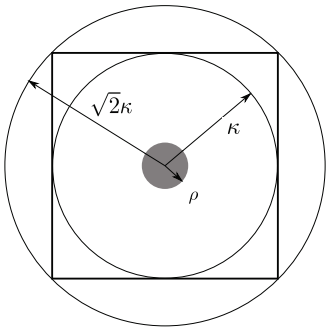

Fig. 2. We approximate the square by two circles, one inscribed in the square, and the other circumscribing the square, in order to calculate bounds on the hitting time.

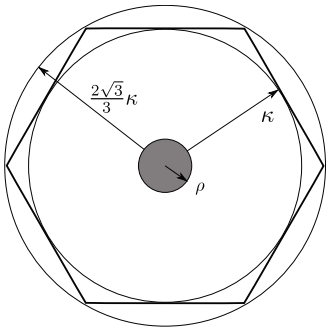

Fig. 3. We approximate the hexagon by two circles, one inscribed in the hexagon, and the other circumscribing the hexagon, in order to calculate bounds on the hitting time.

our derivation and analysis, we first observe the symmetric structures of the square and hexagon grid deployments: as a mobile node reaches the edge of a square or an hexagon, there is no difference between approaching a new communication disk (i.e., coverage area), or returning to the same communication disk, in terms of the time spent outside of coverage areas. Therefore, in our analysis, we restrict our focus to one square in the square grid deployment and to one hexagon in the hexagon deployment.

In this work, we use 2-D Brownian Motion to model the movement of the mobile nodes. We define the hitting time as the time it takes a mobile node just left the edge of the coverage area to hit the edge of the square or hexagon and then to hit (return to) the coverage area again.

Recall that the coverage area has a circular shape and the boundary region has either a square or an hexagonal shape. Therefore, instead of directly calculating the hitting time, we provide a lower and an upper bounds on it. We first derive a lower bound by considering a mobile node traveling in the circle inscribed in the square (Fig. 2) or in the hexagon (Fig. 3) with radius κ and centered at our access point. Similarly, we find an upper bound on the hitting time by considering a mobile node traveling in the outer circle that circumscribes the square or hexagon. In the case of the square grid, this circle has radius $\sqrt{2}\kappa$ and in the case of the hexagon grid, this circle has radius $2\sqrt{3}\kappa/3$, as shown respectively in Figs 2 and 3.

Proposition 3.1: For sufficiently small η, the expected hitting time $\bar{\sigma}$ in the square grid deployment is lower and upper bounded as

$$\kappa^2 \ln\left(\frac{\kappa}{\rho}\right) \leq \bar{\sigma} \leq 2\kappa^2 \ln\left(\frac{\sqrt{2}\kappa}{\rho}\right) \tag{1}$$

Proof: Using the theorem given in [21], it follows that when the coverage area has circular shape of radius ρ and the boundary region also has circular shape of radius $R > \rho$, the expected hitting time can be expressed as $h(\rho, R) = R^2 \ln\left|\frac{R}{\rho}\right|$. Hence, applying this result to the inner boundary region of radius κ and to the outer boundary region of radius $\sqrt{2}\kappa$, as shown in Fig. 2, the expected hitting time $\bar{\sigma}$ in the square grid deployment can then be lower bounded by $h(\rho, \kappa)$ and upper bounded by $h(\rho, \sqrt{2}\kappa)$. ■

Proposition 3.2: For sufficiently small η, the expected hitting time $\bar{\sigma}$ in the hexagon grid deployment is lower and upper bounded as

$$\kappa^2 \ln\left(\frac{\kappa}{\rho}\right) \leq \bar{\sigma} \leq \frac{4}{3}\kappa^2 \ln\left(\frac{2\kappa}{\sqrt{3}\rho}\right) \tag{2}$$

Proof: Similar to the previous proof, provided that the expected hitting time, when the coverage area has circular shape of radius ρ and the boundary region has circular shape of radius $R > \rho$, can be expressed as $h(\rho, R) = R^2 \ln\left|\frac{R}{\rho}\right|$, the expected hitting time $\bar{\sigma}$ in the hexagon grid deployment can be lower bounded by $h(\rho, \kappa)$ and upper bounded by $h(\rho, 2\sqrt{3}\kappa/3)$. ■

A. Sufficient access-point density of square deployment

Recall that $\nu = \frac{1}{4\kappa^2}$ denotes the access-point density of the square grid deployment. We now provide a sufficient condition on the critical density when deploying the access points in the square grid structure.

Theorem 3.3: For sufficiently small ρ, when $\tau \geq \frac{\pi\rho^2}{8}$, the data loss rate is guaranteed to remain below the threshold, $\bar{\epsilon}$, if the following condition on access-point density holds:

$$\nu \geq \frac{-\pi - 2\ln\frac{1}{\bar{\epsilon}} + \sqrt{\left(\pi + 2\ln\frac{1}{\bar{\epsilon}}\right)^2 + 8\left(\frac{4\tau}{\rho^2} - \pi\right)\ln\frac{1}{\bar{\epsilon}}}}{16\tau - 4\rho^2\pi}$$

Proof: Recall that because of symmetry, it suffices to consider the motion of a mobile node on a single square of the grid. Let C be a random variable representing the amount of time the mobile node spends inside the communication disk of radius ρ (i.e., inside the coverage area), and T be a random variable representing the total amount of time spent inside the square of length 2κ. For small coverage ratio η, we can write $\eta \approx \mathbb{E}C/\bar{\sigma}$ or equivalently $\mathbb{E}C \approx \eta\bar{\sigma}$, where $\bar{\sigma}$ is the expected hitting

time and $\mathbb{E}C$ is the expectation of C; i.e., the mean time a mobile node spends in the coverage area.

Now, note that buffer overflow occurs when T minus $\mathbb{E}C$ exceeds τ. Hence, the probability of overflow, P_O, can be expressed as $P(T-\mathbb{E}C > \tau)$ or $P(T > \tau+\mathbb{E}C)$. Since T can be approximated with an exponential distribution with parameter $1/\bar{\sigma}$ [22], P_O can then be written as

$$P_O = \exp\left\{-\frac{\tau}{\bar{\sigma}} - \pi\rho^2\nu\right\} = \exp\left\{-\frac{\tau}{\bar{\sigma}} - \frac{\pi\rho^2}{4\kappa^2}\right\}.$$

From Proposition 3.1, it then follows that the probability of overflow, P_O, is bounded below by

$$\exp\left\{-\frac{\tau}{h(\rho,\kappa)} - \frac{\pi\rho^2}{4\kappa^2}\right\},$$

and bounded above by

$$\exp\left\{-\frac{\tau}{h(\rho,\sqrt{2}\kappa)} - \frac{\pi\rho^2}{4\kappa^2}\right\}.$$

where again $h(x,y) = y^2 \ln\left|\frac{y}{x}\right|$.

We know that for all $z > 0$, $\ln z \leq z-1$ holds, so it then follows that $h(\rho,\sqrt{2}\kappa) \leq f(\rho,\sqrt{2}\kappa)$, where,

$$f(\rho,\sqrt{2}\kappa) = \kappa^2\left(\frac{2\kappa^2}{\rho^2} - 1\right),$$

which implies that

$$\exp\left\{-\frac{\tau}{h(\rho,\sqrt{2}\kappa)} - \frac{\pi\rho^2}{4\kappa^2}\right\} \leq \exp\left\{-\frac{\tau}{f(\rho,\sqrt{2}\kappa)} - \frac{\pi\rho^2}{4\kappa^2}\right\}. \tag{3}$$

Eq. (3) implies that the probability of overflow is also bounded above by

$$\exp\left\{-\frac{\tau}{f(\rho,\sqrt{2}\kappa)} - \frac{\pi\rho^2}{4\kappa^2}\right\}.$$

To ensure that the probability of overflow does not exceed the data loss rate threshold $\bar{\epsilon}$, it suffices then that

$$\exp\left\{-\frac{\tau}{f(\rho,\sqrt{2}\kappa)} - \frac{\pi\rho^2}{4\kappa^2}\right\} \leq \bar{\epsilon}.$$

For $\tau \geq \frac{\pi\rho^2}{8}$, replacing κ^2 by $\frac{1}{4\nu}$ yields (after some algebraic simplification),

$$\left(8\tau\rho^2 - 2\rho^4\pi\right)\nu^2 + \left(\pi\rho^2 + 2\rho^2\ln\frac{1}{\bar{\epsilon}}\right)\nu - \ln\frac{1}{\bar{\epsilon}} \geq 0.$$

Solving the quadratic equation provides the sufficient condition on ν proposed in the theorem for square grid deployment. ■

B. Sufficient access-point density of hexagon deployment

Now, we apply the same approach to derive a sufficient condition on the access-point density for the case of hexagon grid deployment. Recall that in the hexagonal deployment, the access-point density ν can be expressed as $\frac{1}{2\sqrt{3}\kappa^2}$ (as mentioned in Section II).

Theorem 3.4: For a sufficiently small ρ, when $\tau \geq (\pi\rho^2)/(6\sqrt{3})$, data loss rates are guaranteed to remain below a given threshold, $\bar{\epsilon}$, if the following condition on access-point density holds:

$$\nu \geq \frac{-2\pi - 3\sqrt{3}\ln\frac{1}{\bar{\epsilon}}}{54\tau - 6\sqrt{3}\rho^2\pi} + \frac{\sqrt{\left(2\pi + 3\sqrt{3}\ln\frac{1}{\bar{\epsilon}}\right)^2 + 24\sqrt{3}\left(\frac{2\sqrt{3}\tau}{\rho^2} - \pi\right)\ln\frac{1}{\bar{\epsilon}}}}{54\tau - 6\sqrt{3}\rho^2\pi}.$$

Proof: Following similar derivation to that given in the proof of Theorem 3.3 above, P_O can be written as

$$P_O = \exp\left\{-\frac{\tau}{\bar{\sigma}} - \frac{\pi\rho^2}{2\sqrt{3}\kappa^2}\right\}.$$

Now from Proposition 3.2, it follows that P_O is bounded below by

$$\exp\left\{-\frac{\tau}{h(\rho,\kappa)} - \frac{\pi\rho^2}{2\sqrt{3}\kappa^2}\right\},$$

and bounded above by

$$\exp\left\{-\frac{\tau}{h(\rho,\frac{2\sqrt{3}}{3}\kappa)} - \frac{\pi\rho^2}{2\sqrt{3}\kappa^2}\right\}.$$

where again $h(x,y) = y^2\ln\left|\frac{y}{x}\right|$.

Again, as $\ln z \leq z-1$ holds for all $z > 0$, it then follows that $h(\rho,\kappa) \leq f(\rho,\kappa)$ where

$$f\left(\rho,\frac{2\sqrt{3}}{3}\kappa\right) = \frac{2\kappa^2}{3}\left(\frac{4\kappa^2}{3\rho^2} - 1\right),$$

which implies that

$$\exp\left\{-\frac{\tau}{h(\rho,\frac{2\sqrt{3}}{3}\kappa)} - \frac{\pi\rho^2}{2\sqrt{3}\kappa^2}\right\} \leq \exp\left\{-\frac{\tau}{f(\rho,\frac{2\sqrt{3}}{3}\kappa)} - \frac{\pi\rho^2}{2\sqrt{3}\kappa^2}\right\}. \tag{4}$$

Eq. (4) implies that P_O is also bounded above by

$$\exp\left\{-\frac{\tau}{f(\rho,\frac{2\sqrt{3}}{3}\kappa)} - \frac{\pi\rho^2}{2\sqrt{3}\kappa^2}\right\}.$$

To keep the probability of overflow from exceeding the data loss rate threshold $\bar{\epsilon}$, it also suffices that the above bound to be less than or equal to $\bar{\epsilon}$. Then, replacing κ^2 by

its expression $\frac{1}{2\sqrt{3}\nu}$, after some algebra, it yields that for $\tau \geq \frac{\pi\rho^2}{6\sqrt{3}}$,

$$\left(27\tau\rho^2 - 3\sqrt{3}\rho^4\pi\right)\nu^2 + \left(2\pi\rho^2 + 3\sqrt{3}\rho^2 \ln\frac{1}{\bar{\epsilon}}\right)\nu - 2\ln\frac{1}{\bar{\epsilon}} \geq 0. \quad (5)$$

Solving the quadratic equation again provides the stated sufficient condition on ν for hexagonal access-point deployment. ■

C. Asymptotic Analysis

We are also interested in studying the asymptotic behaviors of the access-point density for the studied DTNs. Note that to ensure that the probability of overflow does not exceed the required threshold, it suffices that the density remains below a certain value; which we derived and proposed in Theorems 3.3 and 3.4—we call this value the sufficient access-point density and denote it as ν^s. Note that ν^s depends on the communication radius ρ, the time to overflow the buffer τ, and the given threshold $\bar{\epsilon}$.

Corollary 3.5: For fixed $\bar{\epsilon}$, the sufficient density ν^s in both the square and hexagon grid deployments is $\Theta(1/\sqrt{\tau})$ as $\tau \to \infty$.

Thus for both the square and hexagon deployments, as the buffer size increases to infinity, the sufficient access-point density decreases asymptotically as fast as the inverse of the square root of the buffer size.

Corollary 3.6: For fixed τ, the sufficient density ν^s in both the square and hexagon grid deployments is $\Theta(\ln\frac{1}{\bar{\epsilon}})$ as $\bar{\epsilon} \to 1$.

In other words, as the data loss rate threshold $\bar{\epsilon}$ goes to 1, the sufficient density ν^s decreases asymptotically as fast as $\ln\frac{1}{\bar{\epsilon}}$.

IV. Validation

In this section, we use MATLAB to validate the derived sufficient conditions presented in Theorems 3.3 and 3.4. For this, we conduct simulations of 2-D Brownian motion in the bounded square and hexagonal regions (as shown in Fig. 1). We perform this by simulating two random variables at each time step for the distance the mobile node travels in a unit time interval in the x- and y-directions. We then use it to simulate the hitting time as previously defined: the time it takes the Brownian motion to leave a communication disk (i.e., coverage area), having radius ρ centered at the origin, then hit the boundary of the square or hexagon, and then return to the communication disk. The hitting time is in turn used to measure the average data loss rate (ϵ_m), which is a function of the radius of the communication disk ρ, access-point density ν, and time required to overflow the buffer τ. In our simulation, we consider three different values of ρ, ρ = 30, 20, and 10. We also consider different values of ν (which depends only on κ) for measuring the average data loss rate (for each ρ). We set the data loss rate threshold $\bar{\epsilon} = 0.9$ for each of the two grid deployments. For a given ρ, we calculate the value of τ as $\tau = \pi\rho^2/8$ for square deployment and $\tau = \pi\rho^2/(6\sqrt{3})$ for the hexagon deployment (for both cases, it is notable from Theorem 3.3 and Theorem 3.4 that for a given ρ, any two fixed values greater than the above values can be used). Also, for a fixed ρ, from the Theorem 3.3 and Theorem 3.4, we calculate the theoretical sufficient density, ν^s, which is a function of ρ, τ, and $\bar{\epsilon}$. For each ν^s, we simulate and measure the average data loss rate for various values of ν.

Figs. 4 and 5 illustrate the validation of Theorems 3.3 and 3.4. There are three observations that we make from these two figures. First, observe that when ν is higher than the theoretical sufficient density, ν^s, the measured average data loss rate is blow the given threshold, regardless of the deployment structure. Second, also observe that when the measured data loss rate is above the given threshold, then the corresponding density violates the sufficient density condition. For example, the first bar from the right (in both figures) corresponds to a measured data loss rate that exceeds the threshold, but note that the corresponding density ν does not meet the sufficient density condition either; i.e., $\nu = 0.5\nu^s < \nu^s$. Third, note that when ν is lower than the sufficient density, ν^s, the average data loss rate may or may not exceed the given threshold, since our derived conditions are sufficient. For example, the measured data loss rate exceeds the required threshold in the case of square grid deployment, as shown in Fig. 4 for $\nu = 0.8\nu^s$ (second bar from the right) and $\nu^s = 0.8165 \times 10^4$. Whereas, the measured data loss rate does not exceed the threshold in the case of hexagon grid deployment even when $\nu = 0.8\nu^s$, as shown in Fig. 5 for $\nu^s = 1.084 \times 10^4$. This means, as mentioned earlier, that the conditions provided in the theorems are sufficient, but not necessary.

V. Conclusion

In this paper, we derived and provided sufficient conditions on the density of access-points of DTNs used specifically for wildlife tracking. We also analyzed the asymptotic density behavior under various design parameters. Finally, we validated our models via simulations.

References

[1] M. Rutishauser, V.V. Petkov, T. Williams, C. Wilmers, J. Boice, K. Obraczka, and P. Mantey, "CARNIVORE: A Disruption-Tolerant System for Studying Wildlife," in *Proc. of 19th Int'l Conf. on Computer Communications and Networks*, 2010, pp. 1–8.

[2] A. Mainwaring, D. Culler, J. Polastre, R. Szewczyk, and J. Anderson, "Wireless sensor networks for habitat monitoring," in *Proc. of the 1st ACM international workshop on Wireless Sensor Networks and Applications*, 2002, pp. 88–97.

[3] P. Juang, H. Oki, Y. Wang, M. Martonosi, L.S. Peh, and D. Rubenstein, "Energy-efficient computing for wildlife tracking: Design tradeoffs and early experiences with zebranet," in *ACM SIGOPS Operating Systems Review*, 2002, vol. 36, pp. 96–107.

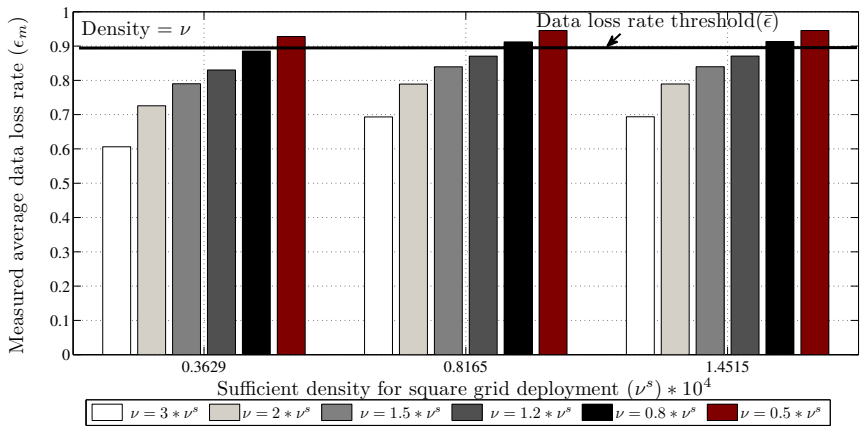

Fig. 4. The measured average data loss rate for various sufficient densities in the square grid deployment

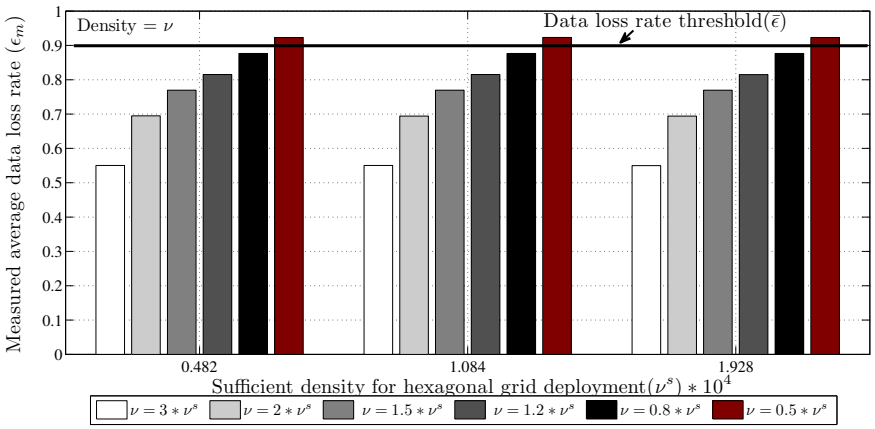

Fig. 5. The measured average data loss rate for various sufficient densities in the hexagon grid deployment

[4] T. Small and Z.J. Haas, "Resource and performance tradeoffs in delay-tolerant wireless networks," in *Proc. of ACM SIGCOMM Workshop on Delay-Tolerant Networking*, 2005, pp. 260–267.

[5] J-H. Huang, Y-Y. Chen, Y-T. Huang, P-Y. Lin, Y-C. Chen, Y-F. Lin, S-C. Yen, P. Huang, and L-J. Chen, "Rapid Prototyping for Wildlife and Ecological Monitoring," *IEEE Systems Journal*, vol. 4, no. 2, pp. 198–209, 2010.

[6] T. El Salti, N. Nasser, T. Taleb, and A. Al-Yatama, "Enhanced topological graphs for 2-d sensor networks," in *Proc. of IEEE ICC*, May 2010.

[7] M. Rahman, N. Nasser, and T. Taleb, "Pairing-based secure timing synchronization for heterogeneous sensor networks," in *Proc. of IEEE GLOBECOM*, Dec. 2008.

[8] T. Taleb, F. Nait-Abdesselam, A. Jamalipour, K. Hashimoto, N. Kato, and Y. Nemoto, "Sat05-1: Design guidelines for a gloal and self-managed LEO satellites-based sensor network," in *Proc. of IEEE GLOBECOM*, Dec. 2006.

[9] N. Chakchouk, B. Hamdaoui, and M. Frikha, "WCDS-DCR: an energy-efficient data-centric routing scheme for wireless sensor networks," *Wireless Comm. and Mobile Computing J., To appear*.

[10] S. Ehsan and B. Hamdaoui, "A survey on energy-efficient routing techniques with QoS assurances for wireless multimedia sensor networks," *IEEE Communications Surveys and Tutorials, To appear*.

[11] Q. Li, S. Zhu, and G. Cao, "Routing in socially selfish delay tolerant networks," in *Proc. of IEEE INFOCOM*, 2010, pp. 1–9.

[12] T. Spyropoulos, T. Turletti, and K. Obraczka, "Routing in delay-tolerant networks comprising heterogeneous node populations," *IEEE Tran. on Mobile Computing*, pp. 1132–1147, 2009.

[13] S. Ehsan, B. Hamdaoui, and M. Guizani, "Cross-layer aware routing approaches for lifetime maximization in rate-constrained wireless sensor networks," in *Proc. of IEEE GLOBECOM*, 2010.

[14] S. Ehsan, B. Hamdaoui, and M. Guizani, "Feasibility conditions for rate-constrained routing in power-limited multichannel WSNs," in *Proc. of IEEE GLOBECOM*, 2011.

[15] F. De Pellegrini, D. Miorandi, I. Carreras, and I. Chlamtac, "A graph-based model for disconnected ad hoc networks," in *Proc. of IEEE INFOCOM*, 2007, pp. 373–381.

[16] Z. Kong and E.M. Yeh, "Connectivity and latency in large-scale wireless networks with unreliable links," in *Proc. of IEEE INFOCOM*, 2008, pp. 11–15.

[17] R. La, "Distributional Convergence of Inter-Meeting Times Under Generalized Hybrid Random Walk Mobility Model," *IEEE Tran. on Mobile Computing*, 2010.

[18] P. Jacquet, B. Mans, and G. Rodolakis, "On space-time capacity limits in mobile and delay tolerant networks," in *Proc. of IEEE INFOCOM*, 2010, pp. 1–9.

[19] M. Garetto, P. Giaccone, and E. Leonardi, "On the capacity of ad hoc wireless networks under general node mobility," in *Proc. of INFOCOM*, 2007, pp. 357–365.

[20] M. Abdelmoumen, E. Dhib, M. Frikha, and T. Chahed, "Impact of mobility patterns on the performance of routing protocols in delay tolerant networks," in *Internal Report, SupCom*, June 2010.

[21] K. Bradford, M.Brugger, S. Ehsan, B. Hamdaoui, and Y. Kovchegov, "Data loss modeling and analysis in partially-covered delay tolerant networks," in *Proc. of IEEE ICCCN*, 2011.

[22] D.J. Aldous, *Probability approximations via the Poisson clumping heuristic*, Springer-Verlag New York, 1988.